Real-World License Plate Image Super-Resolution via Domain-specific Degradation Modeling

Xin Luo
East China Normal University
Shanghai, China
xinluo@stu.ecnu.edu.cn

Yihao Huang
Nanyang Technological University
Singapore
huangyihao22@gmail.com

Weikai Miao*
East China Normal University
Shanghai, China
wkmiao@sei.ecnu.edu.cn

***Abstract*—License plate (LP) recognition systems often struggle to accurately recognize images in complex environments. Recent studies have attempted to improve recognition accuracy by utilizing super-resolution (SR) technology. However, these approaches often fall short in terms of generalization performance, as they rarely consider the various degradations present in real-world images. In this paper, we propose to generate realistic degraded LP images by applying a degradation model on a high-resolution LP dataset, which can cover a wide range of the degradation variations of real-world LP images flexibly. The SR model trained with simulated degraded images has better generalization and robustness on real-world LP images. Experimental evaluations conducted on LP recognition benchmark datasets demonstrate that the proposed method not only produces visually superior results but also effectively improves recognition accuracy.**

***Index Terms*—license plate super-resolution, recognition, real-world, degradation model, high-resolution dataset**

I. Introduction

License plate recognition (LPR) has attracted significant interest in computer vision due to its wide range of practical applications, such as traffic management, security monitoring, and intelligent parking. While LPR systems have made remarkable progress through deep learning, the recognition accuracy of these methods rapidly decreases when faced with low-quality images captured from the real world.

License plate super-resolution (LPSR) was first proposed in [1] to improve recognition accuracy. However, existing LPSR methods [2]–[5] still cannot effectively solve real-world LPSR tasks since they rarely consider the various degradations in real-world LP images. Recently, the blind SR methods like BSRGAN [6] and Real-ESRGAN [7] for the general domain have explored real-world SR and demonstrated their excellent performance in dealing with low-quality degraded images.

An intuitive idea is adopting the blind SR methods into the LPSR task. However, there is a severe transferability problem that the degradation types considered in blind SR methods do not match the LPSR domain. In order to solve the real-world LPSR problem, building a low-resolution LP dataset with domain-specific degradations is a promising method since the generalization of neural networks in the target domain can be improved by this dataset. Directly using the camera to capture low-resolution LP images with various degradation is very difficult and resource-consuming. So we propose to generate a realistic degraded image dataset with a high-resolution LP image dataset and the LP degradation model.

With respect to the high-resolution LP image dataset, natural scenes high-resolution datasets (*e.g.*, DIV2K [8] and Flickr2K [9]) lack unique features of LP shapes, numbers, and characters. Meanwhile, existing real-world LP datasets contain various degradations, and there is no corresponding high-resolution LP image with high fidelity. Thus we build a high-resolution LP dataset termed HRLPD to meet this requirement. The HRLPD dataset consists of 100 high-resolution (2K) images, and we expand it to 5,000 by data augmentation methods such as rotation, cropping, and scaling. Given the high-resolution image from the HRLPD dataset, the corresponding degraded image can be generated by the LP degradation model.

With respect to the LP degradation model, according to the statistical results of the degradation distribution of the existing real-world LP datasets, our proposed LP degradation model consists of motion blur, lighting, Gaussian blur, resizing, and noise, in which motion blur and lighting commonly exist in driving scene and have not been considered in general real-world SR works [6], [7]. Thus we refer to the physical procedure of motion blur and lighting to effectively simulate them in the degradation model. Specifically, the motion blur is achieved by point spread functions with random linear or non-linear motion trajectories. The lighting is realized by simulating the rendering of ambient light, parallel light, and spotlight on the LP image. Considering the uncertainties in the occurrence of degradation in the real world, we adopt a random degradation shuffle sequence proposed by BSRGAN [6] and control the execution of all the degradation by a probabilistic hyperparameter.

We evaluate the model trained by our self-built datasets on three other real-world LP datasets, including CCPD [10], AOLP [11], and RodoSol-ALPR [12]. Meanwhile, we adopt the LP recognition accuracy metric that is commonly used in the LPSR methods [2]–[5]. In summary, our contributions can be summarized in three-fold:

1. To solve the real-world LPSR task, we are the first to propose a complete and domain-specific LP degradation simulation model by introducing motion blur and lighting degradation into the blind SR method.

2. We build a high-resolution LP dataset and combine it with

*Weikai Miao is the corresponding author (wkmiao@sei.ecnu.edu.cn).

979-8-3503-5409-6/24/$31.00 ©2024 IEEE
DOI 10.1109/CAI59869.2024.00210

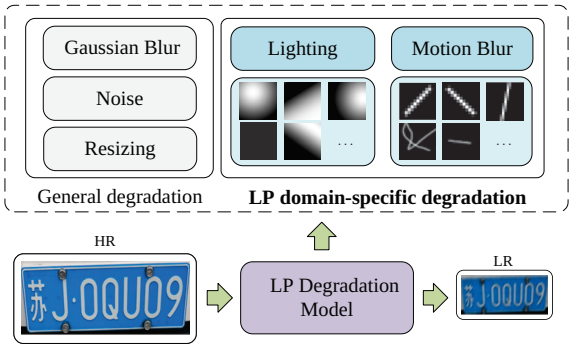

Fig. 1. The whole process of data synthesis, the LP degradation model employs motion blur and light degradation in addition to the general degradation.

the proposed degradation model to generate realistic degraded LP images.

3. Experiments show that the model trained by the self-built dataset produces better visual results and can effectively improve the accuracy of LP recognition in various complex environments.

II. Related Work

A. Blind Super-Resolution

Blind SR is a challenging task that requires simultaneously solving image restoration and SR problems without prior knowledge of the blur kernel. The methods like SRMD [13] and UDVD [14] use the degradation information and LR image as input to the SR model, effectively addressing multiple types of degradation by adapting to the degradation features. However, incorrect estimation of degradation information can cause blurring and unnatural texture details in the super-resolved images. As a remedy, IKC [15] and DAN [16] propose to correct the kernel estimate in an iterative manner. Similarly, KMSR [17] and RealSR [18] propose to estimate kernels from LR images captured in real-world scenes. However, they fail to produce satisfactory results when dealing with degraded images not covered by their models, which is far from generalizing to real-world scenes. To address this issue, recent research has focused on modeling degradation behavior to cover most degradation scenarios in real-world images. For example, BSRGAN [6] proposes a random degradation shuffle sequence and some practical degradation types. Real-ESRGAN [7] proposes a higher-order degradation model to expand the degradation space. Despite their significant progress in improving the perceptual quality of real-world images, they are unsuitable for images in some specific fields (*e.g.*, LP images) since they lack domain-specific degradation types and fail to capture domain-specific texture features.

B. License Plate Super-Resolution

Early works [1], [19], [20] in LPSR mainly relied on traditional image processing methods. The LPSR method has made significant progress benefiting from the development of deep learning. For example, Lai *et al.* [21] uses generative adversarial networks (GANs) with perceptual loss to reconstruct the HR LP images. Zou *et al.* [22] propose an LPSR algorithm based on character semantics. However, their method assumes that the LR image is generated by bicubic interpolation downsampling of the HR image, which is impractical in real-world images. For realistic scenarios, Liu *et al.* [4] propose using GANs to extract complementary information from multiple images to recover the LP number. Zhang *et al.* [5] adopt the prior knowledge of LP to generate the spatial corresponding HR images. However, they cannot be generalized to wider real-world scenarios since most of them do not consider various degradation factors in the real world. Recently, researchers have started to consider the LP image degradation issue. For example, Hamdi *et al.* [2] adopt a style translation network to distort images. Nascimento *et al.* [23] propose to degrade HR images by iteratively applying random Gaussian noise. However, simple degradation methods can only cover limited scenarios, and unsuitable degradation will produce severe artifacts.

III. Methodology

A. The Real-world License Plate Degradation

Before providing our LP degradation model, we collected and analyzed degradation types distributed in six real-world LP datasets. We divide these degradations into the following four types: Gaussian blur, motion blur, noise, and lighting. The LPR systems often fail to correctly recognize low-quantity LP images with these degradation types. The statistical results are shown in Table I.

TABLE I
Degradations in six real-world LP datasets.

Dataset	Gaussian	Motion	Noise	Lighting
EnglishLP [24]	✓	✗	✓	✓
ChineseLP [25]	✓	✓	✓	✓
AOLP [11]	✓	✓	✓	✓
UFPR-ALPR [26]	✓	✗	✓	✗
CCPD [10]	✓	✓	✓	✓
RodoSol-ALPR [12]	✓	✓	✓	✓

Gaussian blur. Blurring in the real world is usually caused by a variety of factors, such as improper focus, camera lens distortion, *etc*. The LP capturing scene also suffered from this degradation as other common scenes.

Motion blur. Motion blur occurs when an object is moving too fast or the camera shakes, which commonly exists in the process of photographing LP images. This degradation causes numbers and characters to appear ghosting on the LP image, making edge detail difficult to discern.

Noise. Noise refers to irregular isolated pixels that interfere with the observable information of an image. Influenced by camera sensor material, operating environment, *etc.*, various noises will be introduced during image acquisition. Unpleasant blocking artifacts can also be introduced during image compression or transmission. This degradation also occurs frequently in LP images.

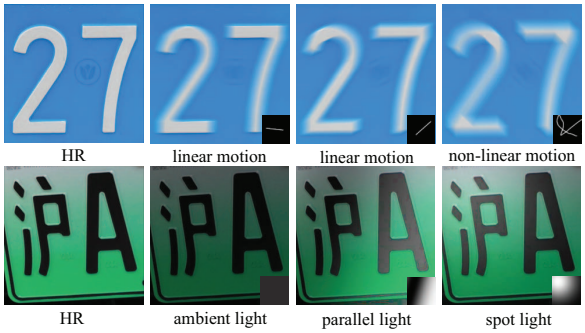

Fig. 2. **Top:** The visualization of the motion kernel and the corresponding blurred image. **Bottom:** The visualization of the light mask image and the corresponding rendered image.

Lighting. Unsuitable lighting will degrade the quality of LP images. Specifically, low-contrast scenes result in images with less detail, which is challenging to analyze and interpret. Imaging under excessive lighting conditions may result in a loss of highlight detail. Uneven lighting scenes can cause shadows and color distortions in LP images. Different types of lights in the real world produce different color temperatures and tints, which can also cause color distortion or white balance problems.

B. The License Plate Degradation Model

Based on the above survey, we propose a complete and domain-specific LP degradation model. The whole pipeline of data synthesis is shown in Fig. 1. For the degradation process, we not only adopt the practical degradation types (*i.e.*, Gaussian blur, noise, and resizing), but also additionally employ motion blur and lighting degradation in the LP degradation model. Considering the uncertainties in the occurrence of degradation in the real world, we control the execution of all the degradations via a probability hyper-parameter. In the LR image synthesis procedure, we apply this LP degradation model on the high-resolution LP dataset proposed in Sec. III-C to generate realistic degraded images.

Motion blur simulation. The physical modeling of motion blur can be described by a point spread function (PSF). During a moving object forms an image on the photosensitive element, since the object has moved a certain distance before the shutter closes, the formed pattern appears as one or some tracks. The spatial distribution of tracks on the photosensitive element is the PSF. A motion-blurred image can be modeled by

$$\mathbf{Y} = \mathrm{PSF} * \mathbf{X} + \mathbf{N} \tag{1}$$

where $\mathbf{Y}$ is a motion-blurred image, $\mathbf{X}$ is the sharp latent image, $*$ denote the convolution operator, $\mathbf{N}$ is additive noise.

The classical motion deblurring work [27]–[29] usually assumes the PSF is linear motion, which may reduce the quality of the latent image since the natural motion blur may be caused by non-linear motion. [30], [31] adopt random motion trajectories to achieve non-linear motion blur. Since real-world motion blur parameters are unknown, we model motion blur as the convolution with a PSF of random linear or non-linear motion trajectories. A visualization of the motion blur kernel is shown in Fig 2 (Top).

Lighting simulation. We simulate three light effects with different properties in the real world, including ambient light, parallel light, and spotlight. Specifically, ambient light means that the light intensity is the same everywhere in space, parallel light refers to multiple light sources illuminating the same direction in parallel, and the spotlight is a light source that emanates from a point. Following the fact that the light intensity will attenuate with the increase of the spatial distance, we use a Gaussian distribution to simulate the trend of light attenuation (as shown in Eq. 2). For ambient light, we generate a completely black or white light mask. For parallel light or spotlight, we first randomly select the position of the light source and then generate a light mask according to the attenuation characteristics (*i.e.* direction) of the light source. We randomly select a lighting effect and merge its resulting light mask with the HSV space of the image with different weights to simulate real-world lighting. A visualization of the light mask image is shown in Fig 2 (Bottom).

$$L_i = L_{max} \cdot \exp\left(-\frac{(d_i - \mu)^2}{\sigma^2}\right) \tag{2}$$

where L_i is the brightness value at position i, L_{max} is the maximum value of brightness, d_i is the distance from the position of i to the light source, μ and σ are the mean and variance of the Gaussian distribution, respectively, which are associated with lighting effect and the size of the image.

C. The High-Resolution License Plate Dataset

Existing public LP datasets (*e.g.*, AOLP [11], CCPD [10]) contain various degradations while lacking corresponding non-degradation HR images. Thus we can not collect LR-HR image pairs for LPSR tasks in the real world with them. To fill this gap, we establish a high-quality (*i.e.*, minor degradation) and high-resolution LP dataset called HRLPD. We select 100 images with higher quality from 200 captured images by Laplacian blur detection [32], where each image was captured by a Canon EOS M100 camera with a resolution of 2460 $\times$ 1680. Specifically, this dataset was shot under good illumination, and we fixed the camera during imaging to prevent subtle shakes caused by manual shooting. The HRLPD dataset contains three types of Chinese LP images, including new energy vehicles (green), fuel vehicles (blue), and large vehicles (yellow). A small sample of images from the HRLPD dataset is shown in Fig. 3. Following the practice in blind SR work [6], [7], we use data augmentation techniques (*e.g.*, flipping, random cropping, and warping) to generate 5,000 HR patch images with 256 $\times$ 256 resolution. The experiments have proven that training using this dataset can better capture the texture features of LP images.

Fig. 3. A small sample of images from the HRLPD dataset.

IV. Experiments

A. Training Details and Evaluation

Datasets. We first train the SR model using DIV2K [8] and Flickr2K [9], which are high-quality (2K resolution) datasets widely used for image restoration tasks. Then we fine-tune the model by HRLPD dataset. The training LR patch size is 64 $\times$ 64, and the LR image is generated by the LP degradation model. We evaluate our method on three real-world LP datasets with different degradation distributions, including AOLP [11], CCPD [10], and RodoSol-ALPR [12]. The AOLP consists of 2,049 images collected in Taiwan, CCPD consists of over 250k Chinese blue and green LP images, RodoSol-ALPR consists of 20,000 Brazilian LP images, where AOLP contains slight degradation, CCPD and RodoSol-ALPR include images of different degradation levels and degradation types. We select all images of AOLP and randomly select 2,000 vehicle images from CCPD and Rodosor-ALPR, respectively, as the testing dataset.

Training details. Our innovation is mainly the LP domain degradation model, we adopt the widely used ESRGAN [33] as the SR model. We train it on HR-LR data pairs generated by applying the LP degradation model on the HRLPD dataset. Meanwhile, we use data augmentation techniques to expand the training dataset and remove some plain background images without characters. The number of training data pairs is 5000, and the execution probability for each degradation type is set to 0.5. We conduct experiments with a scale factor of 4 and performed on two NVIDIA GeForce RTX 3090 GPUs. The model is trained by Adam optimizer. The learning rate is 10^{-4}, the batch size is 16, and the total number of iterations is 400K.

Evaluation. The main purpose of image super-resolution is to improve the accuracy of license plate recognition, so we adopt recognition accuracy as an evaluation. For the LPR system, we choose open source one with excellent performance [34].

B. Compared Methods

We compare the proposed method with LPE [35], BSRGAN [6], Real-ESRGAN [7], MPRNet [36], DeblurGAN [31], SCI [37]. Specifically, LPE is an LPSR method that uses random brightness and noise to degrade the CCPD [10] dataset for training. BSRGAN employs a random degradation shuffle strategy, and Real-ESRGAN proposes a high-order degradation process. The MPRNet, DeblurGAN, and SCI are used for denoising, deblurring, and low-light enhancement, respectively.

TABLE II
Comparison result of different image SR and restoration methods on three real-world LP datasets.

Method	AOLP	CCPD	Rodosol-ALPR
Original	0.9853	0.8430	0.9335
LPE [35]	0.9892	0.8516	0.9382
BSRGAN [6]	0.9922	0.8077	0.9104
Real-ESRGAN [7]	0.9925	0.8120	0.9096
MPRnet [36]	0.9860	0.8443	0.9381
DeblurGAN [31]	0.9594	0.8075	0.9104
SCI [37]	0.9630	0.7720	0.8925
Ours	**0.9956**	**0.8965**	**0.9705**

C. Results on Real-World Dataset

Quantitative results. The results of recognition accuracy are shown in Table II. LPE and MPRNet bring limited improvement. Real-ESRGAN and BSRGAN perform poorly on CCPD [10] and Rodosol-ALPR [12] datasets, mainly because they produce severe artifacts and lose original semantic information when facing unknown degraded inputs. DeblurGAN and SCI also showed declines due to degradation mismatch. The SR models trained with our simulated degradation dataset have better generalization performance on real-world LP datasets. Specifically, our method improves **1.03%** on AOLP, **5.35%** on CCPD, and **3.70%** on Rodosol-ALPR.

Qualitative results. The visual results are shown in Fig. 4. For image restoration methods, MPRNet and DeblurGAN perform unsatisfactorily on low-resolution LP images, SCI only increases the brightness. For image SR methods, it can be observed that LPE fails to remove various blurs and noises. Real-ESRGAN and BSRGAN produce severe artifacts when processing LP images of degradation types not covered in their degradation models. Our model can generate high-quality images with clearly visible edges when treating LP images with multiple degradation types, which shows that the proposed method is robust and effective.

TABLE III
Ablation study on the effectiveness of the different components. **TDY** represents the proposed two degradation types, and **HRLPD** is the proposed high-resolution LP dataset.

Method	AOLP	CCPD	Rodosol-ALPR
Original	0.9853	0.8430	0.9335
w/ TDY w/o HRLPD	0.9505	0.8125	0.8940
w/o TDY w/ HRLPD	0.9922	0.8075	0.9105
w/ TDY w/ HRLPD	**0.9956**	**0.8965**	**0.9705**

D. Ablation Study

We performed an ablation study on two proposed components: a high-resolution LP dataset (**HRLPD**) and two degradation types (**TDY**): illumination and motion blur. We use the image recognition results of degraded low-resolution LP images as the original results. The experimental setup and accuracy results are shown in Table III.

Fig. 4. Qualitative comparisons of different SR methods on real-world LP images with scale factor 4. Better zoom in for details.

The results show that omitting any method component seriously affected the recognition performance. Specifically, the method of not introducing the proposed two degradation types only improves the recognition accuracy on the slightly degraded AOLP [11] dataset. Lack of fine-tuning on the HRLPD dataset leads to a drop in recognition accuracy. The reason may be that using natural scenes for training cannot capture the unique texture features of the LP images, resulting in strange artifacts. This inspires us to design efficient specific solutions for specific domains, rather than general solutions.

E. Visualization of Recognition Results.

In order to demonstrate the effectiveness of this method more intuitively, we show samples of the recognition results of various degraded LP images (all derived from real-world license plate datasets) corrected by our method. As shown in Figure 5, the LPR system incorrectly recognized some characters containing noise and ambiguity, such as ”8” as ”B”, ”E” as ”F”, and the presence of characters that cannot be recognized in low light conditions. Our method removes noise and blur in the image and improves the quality of the image, which can effectively avoid such recognition errors.

V. Conclusion

In this paper, we analyze the degradation types present in real-world LP images and design an LP domain-specific degradation model by introducing motion blur and lighting on traditional degradation types. We applied it to a high-resolution LP dataset to generate realistic degraded images. Although there is still a gap between the hand-designed degradation operator and the real degradation process, the proposed LP degradation model is sufficient for the LPSR task. Our method is easy and effective, the SR model trained on synthetic data has outstanding robustness and generalization on real-world LP datasets, which can produce better visual results and improve the recognition accuracy.

Fig. 5. The sample of correcting the recognition results by the proposed method. Error results are marked in red.

VI. Acknowledgments

The work is supported by the Natural Science Foundation (No.: 62372181).

REFERENCES

[1] Jie Yuan, Si-dan Du, and Xiang Zhu, "Fast super-resolution for license plate image reconstruction," in *CVPR*. IEEE, 2008, pp. 1–4.

[2] Abdelsalam Hamdi, Yee Kit Chan, and Voon Chet Koo, "A new image enhancement and super resolution technique for license plate recognition," *Heliyon*, vol. 7, no. 11, pp. e08341, 2021.

[3] Anwesh Kabiraj, Debojyoti Pal, Debayan Ganguly, Kingshuk C, and Sudipta Roy, "Number plate recognition from enhanced super-resolution using generative adversarial network," *MTA*, vol. 82, no. 9, pp. 13837–13853, 2023.

[4] Wu Liu, Xinchen Liu, Huadomg Ma, and Peng Cheng, "Beyond human-level license plate super-resolution with progressive vehicle search and domain priori gan," in *ACM MM*, 2017, pp. 1618–1626.

[5] Minghui Zhang, Wu Liu, and Huadong Ma, "Joint license plate super-resolution and recognition in one multi-task gan framework," in *ICASSP*. IEEE, 2018, pp. 1443–1447.

[6] Kai Zhang, Jingyun Liang, Luc Van Gool, and Radu Timofte, "Designing a practical degradation model for deep blind image super-resolution," in *ICCV*, 2021, pp. 4791–4800.

[7] Xintao Wang, Liangbin Xie, Chao Dong, and Ying Shan, "Real-esrgan: Training real-world blind super-resolution with pure synthetic data," in *ICCV*, 2021, pp. 1905–1914.

[8] Eirikur Agustsson and Radu Timofte, "Ntire 2017 challenge on single image super-resolution: Dataset and study," in *CVPR*, 2017, pp. 126–135.

[9] Radu Timofte, Eirikur Agustsson, Luc Van Gool, Ming-Hsuan Yang, and Lei Zhang, "Ntire 2017 challenge on single image super-resolution: Methods and results," in *CVPR*, 2017, pp. 114–125.

[10] Zhenbo Xu, Wei Yang, Ajin Meng, Nanxue Lu, Huan H, Changchun Ying, and Liusheng Huang, "Towards end-to-end license plate detection and recognition: A large dataset and baseline," in *ECCV*, 2018, pp. 255–271.

[11] Gee-Sern Hsu, Jiun-Chang Chen, and Yu-Zu Chung, "Application-oriented license plate recognition," *TVT*, vol. 62, no. 2, pp. 552–561, 2012.

[12] Rayson Laroca, Everton V Cardoso, Diego R Lucio, Valter Estevam, and David Menotti, "On the cross-dataset generalization in license plate recognition," *arXiv:2201.00267*, 2022.

[13] Kai Zhang, Wangmeng Zuo, and Lei Zhang, "Learning a single convolutional super-resolution network for multiple degradations," in *CVPR*, 2018, pp. 3262–3271.

[14] Yu-Syuan Xu, Shou T, Yu Tseng, Hsien-Kai Kuo, and Yi-Min Tsai, "Unified dynamic convolutional network for super-resolution with variational degradations," in *CVPR*, 2020, pp. 12496–12505.

[15] Jinjin Gu, Hannan Lu, Wangmeng Zuo, and Chao Dong, "Blind super-resolution with iterative kernel correction," in *CVPR*, 2019, pp. 1604–1613.

[16] Yan Huang, Shang Li, Liang Wang, Tieniu Tan, et al., "Unfolding the alternating optimization for blind super resolution," *NIPS*, vol. 33, pp. 5632–5643, 2020.

[17] Ruofan Zhou and Sabine Susstrunk, "Kernel modeling super-resolution on real low-resolution images," in *ICCV*, 2019, pp. 2433–2443.

[18] Xiaozhong Ji, Yun Cao, Ying Tai, Chengjie Wang, Jilin Li, and Feiyue Huang, "Real-world super-resolution via kernel estimation and noise injection," in *CVPR workshops*, 2020, pp. 466–467.

[19] Menna Ghoneim, Mohamed Rehan, and Hisham Othman, "Using super resolution to enhance license plates recognition accuracy," in *ICCES*. IEEE, 2017, pp. 515–518.

[20] En Wei Zheng and Xian Jun Wang, "An effective regularization method for image super resolution," in *Advanced Materials Research*. Trans Tech Publ, 2011, vol. 219, pp. 1411–1414.

[21] Tan Kean Lai, Aymen F Abbas, Aliyu M Abdu, Usman U Sheikh, Musa Mokji, and Kamal Khalil, "Super resolution of car plate images using generative adversarial networks," in *CSPA*. IEEE, 2019, pp. 80–85.

[22] Yuexian Zou, Yi Wang, Wenjie Guan, and Wenwu Wang, "Semantic super-resolution for extremely low-resolution vehicle license plate," in *ICASSP*. IEEE, 2019, pp. 3772–3776.

[23] Valfride Nascimento, Rayson Laroca, Jorge de A Lambert, William Robson Schwartz, and David Menotti, "Combining attention module and pixel shuffle for license plate super-resolution," *arXiv:2210.16836*, 2022.

[24] Kalafatić Zoran, "Englishlp," https://www.zemris.fer.hr/projects/LicensePlates/english/baza_slika.zip.

[25] Wengang Zhou, Houqiang Li, Yijuan Lu, and Qi Tian, "Principal visual word discovery for automatic license plate detection," *IEEE transactions on image processing*, vol. 21, no. 9, pp. 4269–4279, 2012.

[26] Rayson Laroca, Evair Severo, Luiz A Zanlorensi, Luiz S Oliveira, Gabriel Resende Gonçalves, William Robson Schwartz, and David Menotti, "A robust real-time automatic license plate recognition based on the yolo detector," in *IJCNN*. IEEE, 2018, pp. 1–10.

[27] Jinshan Pan, Zhe Hu, Zhixun Su, and Ming-Hsuan Yang, "Deblurring text images via l0-regularized intensity and gradient prior," in *CVPR*, 2014, pp. 2901–2908.

[28] Jian Sun, Wenfei Cao, Zongben Xu, and Jean Ponce, "Learning a convolutional neural network for non-uniform motion blur removal," in *Proceedings of the IEEE conference on computer vision and pattern recognition*, 2015, pp. 769–777.

[29] Li Xu, Jimmy S Ren, Ce Liu, and Jiaya Jia, "Deep convolutional neural network for image deconvolution," *Advances in neural information processing systems*, vol. 27, 2014.

[30] Ayan Chakrabarti, "A neural approach to blind motion deblurring," in *ECCV*. Springer, 2016, pp. 221–235.

[31] Orest Kupyn, Volodymyr Budzan, Mykola Mykhailych, Dmytro Mishkin, and Jiří Matas, "Deblurgan: Blind motion deblurring using conditional adversarial networks," in *CVPR*, 2018, pp. 8183–8192.

[32] Raghav Bansal, Gaurav Raj, and Tanupriya Choudhury, "Blur image detection using laplacian operator and open-cv," in *SMART*. IEEE, 2016, pp. 63–67.

[33] Xintao Wang, Ke Yu, Shixiang Wu, Jinjin Gu, Yihao Liu, Chao Dong, Yu Qiao, and Chen Change Loy, "Esrgan: Enhanced super-resolution generative adversarial networks," in *ECCV*, 2018, pp. 0–0.

[34] Rayson Laroca, Luiz A Zanlorensi, Gabriel R Gonçalves, Eduardo Todt, William Robson Schwartz, and David Menotti, "An efficient and layout-independent automatic license plate recognition system based on the yolo detector," *IET Intelligent Transport Systems*, vol. 15, no. 4, pp. 483–503, 2021.

[35] Zixuan Zhang and Chengxuan Cai, "License plate enhancement," https://github.com/zzxvictor/License-super-resolution.

[36] Syed Waqas Zamir, Aditya Arora, Salman Khan, Munawar Hayat, Fahad Shahbaz Khan, Ming-Hsuan Yang, and Ling Shao, "Multi-stage progressive image restoration," in *CVPR*, 2021, pp. 14821–14831.

[37] Long Ma, Tengyu Ma, Risheng Liu, Xin Fan, and Zhongxuan Luo, "Toward fast, flexible, and robust low-light image enhancement," in *CVPR*, 2022, pp. 5637–5646.